A NOVEL METHOD FOR SEGMENTATION OF BREAST MASSES BASED ON MAMMOGRAPHY IMAGES

Haichao Cao, Shiliang Pu, and Wenming Tan*

Hikvision Digital Technology Company Limited, Hangzhou 310051, China

2021 IEEE International Conference on Image Processing (ICIP) | 978-1-6654-4115-5/21/$31.00 ©2021 IEEE | DOI: 10.1109/ICIP42928.2021.9506159

ABSTRACT

The accurate segmentation of breast masses in mammography images is a key step in the diagnosis of early breast cancer. To solve the problem of various shapes and sizes of breast masses, this paper proposes a cascaded UNet architecture, which is referred to as CasUNet. CasUNet contains six UNet subnetworks, the network depth increases from 1 to 6, and the output features between adjacent subnetworks are cascaded. Furthermore, we have integrated the channel attention mechanism based on CasUNet, hoping that it can focus on the important feature maps. Aiming at the problem that the edges of irregular breast masses are difficult to segment, a multi-stage cascaded training method is presented, which can gradually expand the context information of breast masses to assist the training of the segmentation model. To alleviate the problem of fewer training samples, a data augmentation method for background migration is proposed. This method transfers the background of the unlabeled samples to the labeled samples through the histogram specification technique, thereby improving the diversity of the training data. The above method has been experimentally verified on two datasets, INbreast and DDSM. Experimental results show that the proposed method can obtain competitive segmentation performance.

Index Terms—deep learning, convolutional neural network, mammography image, breast mass segmentation

1. INTRODUCTION

Breast cancer is one of the most common malignant tumors in women, and it has become a malignant disease affecting women's health and life safety [1]. At present, the incidence of breast cancer in China is increasing year by year, and an average of nearly 180,000 women are diagnosed with breast cancer each year, of which 13,000 women die from breast cancer [2,3]. Clinical studies have shown that if breast mass can be detected early and treated effectively, the mortality rate will be greatly reduced, and the 5-year survival rate can reach 90% [4].

Early detection of breast cancer nowadays tends to carry out by non-invasive medical imaging diagnoses, such as mammography, ultrasound imaging, near infrared scanning, computed tomography imaging and magnetic resonance imaging. Among them, mammography examination is known as the most effective and reliable method for breast cancer examination because of its clear imaging, high image resolution and high sensitivity to early breast masses [5]. In the imaging diagnosis method based on mammography images, accurately segmenting the breast mass is an important step in the early diagnosis of breast cancer, because it can directly affect the subsequent analysis results. With the continuous increase in the number of mammography images, the development of robust segmentation models has important clinical significance to avoid cumbersome manual intervention and improve the repeatability of results [6].

In recent years, scholars at home and abroad have made a lot of research on breast mass segmentation tasks, and many methods have been presented. For example, a threshold-based segmentation method [7,8], a region-based segmentation method [9,10], an energy-optimized segmentation method [11,12], and a deep learning-based segmentation method [13–19].

To obtain a robust, deep learning-based breast mass segmentation model, we propose a Cascaded UNet (CasUNet) network architecture, which is suitable for the segmentation of various types of breast masses. Our contributions are summarized as below:

(1) The CasUNet architecture cascades six UNet [20] sub-networks with increasing depth, which can effectively extract semantic features at different levels and can better adapt to the heterogeneity of breast masses.

(2) To ensure the diversity of training data, a background migration data augmentation method based on histogram specification technology is presented to make better use of the background information of unlabeled data.

(3) To obtain more accurate segmentation results, a multi-stage cascaded training and prediction method is proposed, so that the model can gradually refine the segmentation results.

2. PROPOSED METHOD

In this study, the breast mass segmentation method is divided into three modules, which are data augmentation, segmentation network construction, and model training and prediction.

2.1. Background migration

A robust convolutional neural network (CNN) model often relies heavily on the size of the dataset and the diversity of the data. Compared with natural images, the access to medical image data is very limited. Besides, the relevant labels require professional radiologists to label, and even require professional

This work was supported by China Postdoctoral Science Foundation under Grant No. 2020TQ0086.

E-mail: pushiliang.hri@hikvision.com (Shiliang Pu)

methods such as puncture and biopsy to give accurate labels. Especially for medical image segmentation tasks, what the computer needs is not the central coordinates or benign and malignant labels of the lesion, but the position coordinates of all pixels on the boundary of the more complicated lesion. Hence, medical image datasets used for segmentation tasks are generally relatively small, and the diversity of data is also very limited. Therefore, how to expand training data and how to further ensure the diversity of training data has become a key issue in the application of deep learning models in medical image segmentation tasks. At present, many data augmentation methods have been reported [21–23] and common ones include random rotation, random translation, mirroring, and random cropping. Such methods can increase the sample size of the data set to a certain extent, but they cannot guarantee the diversity of training data. Hence, a data augmentation method called background migration is proposed, which can not only effectively expand the training data, but also ensure the diversity of the training data.

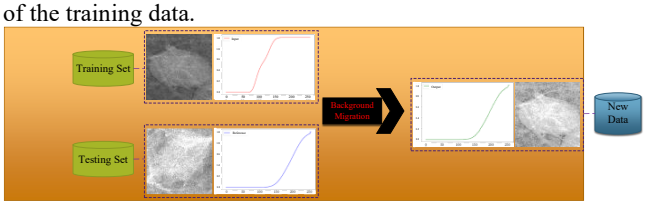

Fig.1. The flowchart of background migration method.

The flowchart of the background migration data augmentation method is shown in **Fig.1**. Specifically, first randomly select a sample from the divided training set as the image to be expanded, called OImg, and then select a sample as the background image to be migrated, called BImg, and finally use the histogram regularization technology [24] for background Migration. In this way, a new image can be obtained, denoted as NImg, the label of NImg is the same as the label of OImg.

2.2. Cascaded UNet architecture

The key to CNN-based segmentation networks is to learn reliable high-resolution features. The CasUNet architecture maintains high-resolution features throughout the process. The CasUNet architecture consists of six cascaded UNet sub-networks, and the depths of these six sub-networks are different, so that it can effectively extract the multi-scale features of breast masses. Next, we have introduced an attention mechanism to enable the model to focus on important information and ignore unimportant information. Specifically, we introduce SeResNet [25] attention mechanism module on the feature maps generated by three UNet sub-networks with depths of 4, 5, and 6. The module automatically obtains the importance of each feature channel through learning, and uses the obtained importance to strengthen effective features and suppress features that are not important to the current task.

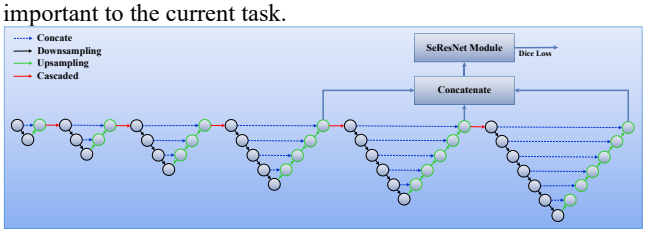

Fig.2. The CasUNet architecture diagram

The schematic diagram of the CasUNet architecture is shown in **Fig.2**. **Table 1** and **Table 2** respectively list the basic structure of the CasUNet and the parameters of each component.

Table 1. The basic structure of the Cascaded UNet architecture. k represents the size of the convolution kernel, and m and n represent the number of input channels and output channels, respectively.

Layer Name	Network Structure
Conv(k, m, n)	[k×k, m, n]
CBlock(c1, c2)	Conv(3, c1, c2), Conv(3, c2, c2)
Down(d1, d2)	CBlock(d1, d2), MaxPool2d(2)
Up(u1, u2)	Upsample(2), Conv(3, u1, u2), CBlock(2*u2, u2), Concatenation

Table 2. Network parameters of the Cascaded UNet architecture. $UNet_i$ means the depth of the UNet subnet is i, and the value in (*) means the parameters required by ConvBlock, Down, Up and Conv. The input channel of the first stage model is 1, and the input channel of the second and third stage models is 2. r represents the reduction ratio in SeResNet.

Layer	$UNet_1$	$UNet_2$	$UNet_3$	$UNet_4$	$UNet_5$	$UNet_6$
CB(c1, c2)	(1, 32)	(32, 32)				
Down(d1, d2)	(32, 64)	(32, 64) (64, 96)	(32, 64) (64, 96) (96, 128)	(32, 64) (64, 96) (96, 128) (128, 160)	(32, 64) (64, 96) (96, 128) (128, 160) (160, 196)	(32, 64) (64, 96) (96, 128) (128, 160) (160, 196) (196, 228)
CBlock(c1, c2)	(64, 64)	(96, 96)	(128, 128)	(160, 160)	(196, 196)	(228, 228)
Up(u1, u2)	(64, 32)	(96, 64) (64, 32)	(128, 96) (96, 64) (64, 32)	(160, 128) (128, 96) (96, 64) (64, 32)	(196, 160) (160, 128) (128, 96) (96, 64) (64, 32)	(228, 196) (196, 160) (160, 128) (128, 96) (96, 64) (64, 32)
Conv(k, m, n)	*	*	*	(1, 32, 1)	(1, 32, 1)	(1, 32, 1)
SeResNet	*	*	*	r=16		

2.3. Multi-stage cascaded training and prediction method

To make better use of the limited training data, a multi-stage cascaded training method is proposed, which can gradually refine the segmentation results. The design idea of this method is: first let the model focus on the characteristics of the learning target itself, and then gradually add certain context information on this basis for fine-tuning. It is like simulating the human learning process, that is, first learn in a simple background, and then gradually transition to a complex background.

The workflow of the multi-stage cascaded training method is as follows:

1) According to the mask images in the training set, three image blocks of different scales are sampled in the intensity image and the mask image to form the training sets T1, T2, and T3. As shown in **Fig.3**, taking the mask image as an example, the size relationships of three different scales (S1, S2, and S3) are respectively shown, and they need to be scaled to 256×256 during training. Where L represents the maximum value of the width and height of the circumscribed rectangle of the breast mass in the mask image;

2) Use the training set T1 corresponding to the small-scale S1 that contains almost no context information to train a small-scale model, denoted as M1; then, use the model M1 to predict the image blocks in the training set T1, so as to obtain the dataset of the predicted mask image corresponding to the small-scale S1 in the first stage, denoted as PM1; after that, use a value of 0 to expand the pictures in PM1 to the same size as the medium-scale S2, and finally scale them all to 256*256.

3) Use the training set T2 corresponding to the medium-scale S2 containing certain context information and the acquired

data set PM1 of the first stage to train a medium-scale model, denoted as M2; when training M2, random elastic deformation [26] is performed on the pictures of the data set PM1 to ensure the diversity of training data and improve the generalization performance of M2. then, use the model M2 to predict the image blocks in the training set T2, so as to obtain the data set of the predicted mask image corresponding to the middle-scale S2 in the second stage, denoted as PM2; after that, use a value of 0 to expand the image in PM2 to the same size as the large-scale S3, and finally scale them all to 256*256.

4) Finally, use the training set T3 corresponding to the large-scale S3 containing rich context information and the data set PM2 obtained in the second stage to train a large-scale model, denoted as M3; similarly, when training M3, the image in PM2 perform random elastic deformation to improve the generalization performance of model M3

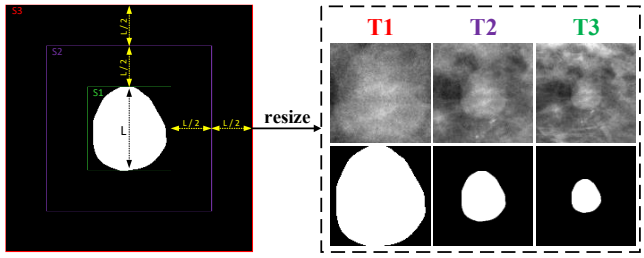

Fig. 3. Example images of training datasets T1, T2 and T3 corresponding to three different scales S1, S2 and S3.

The prediction process of the multi-stage cascade is like the training process, and is also divided into three stages, as shown in **Fig. 4**.

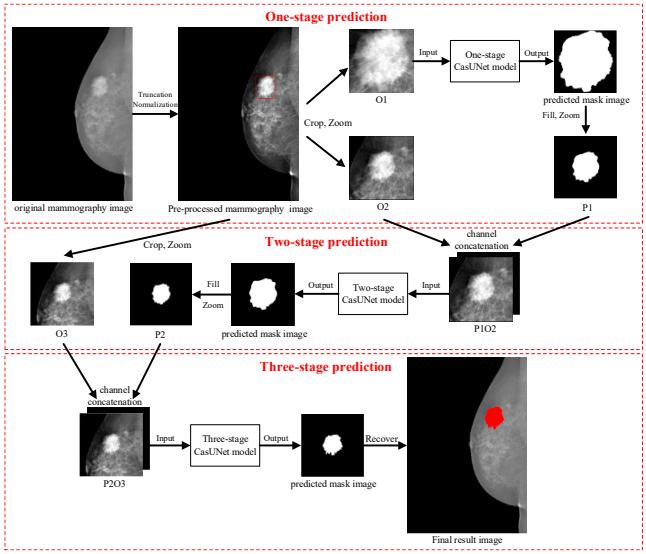

Fig. 4. Schematic diagram of the multi-stage cascaded prediction process

3. EXPERIMENTS

The experimental data used in this study comes from two public data sets: INbreast [27] and DDSM [28]. The INbreast dataset comes from the Breast Center Hospital in Porto, Portugal. There is a total of 410 images, of which the number of images containing breast masses is 116. DDSM data comes from institutions such as Massachusetts General Hospital, Wake Forest University School of Medicine, Sacred Heart Hospital, and University of Washington. It contains 2620 cases, including 695 cases without masses, 1925 cases with masses, and a total of 10480 mammography images.

When evaluating performance, the evaluation indicators we use are IOU (Intersection Over Union), DSC (Dice Similarity Coefficient), REC (Recall), SPC (Specificity) and Haus (Hausdorff). Their definitions are shown in formulas (1)-(5).

$$IOU = (P \bigcap G)/(P \bigcup G) \tag{1}$$

$$DSC = [2 \times S(P \bigcap G)]/[S(P) + S(G)] \tag{2}$$

$$REC = S(P \bigcap G)/S(G) \tag{3}$$

$$REC = S(P \bigcap G)/S(P) \tag{4}$$

$$Haux(P,G) = \max\left\{ \sup_{p \in P} \inf_{g \in G} d(p,g),\ \sup_{g \in G} \inf_{p \in P} d(p,g) \right\} \tag{5}$$

Among them, P represents the predicted mask region, G represents the region corresponding to the ground truth, S(*) represents the area counted in pixels, and d(i, j) represents the Euclidean distance between pixels i and j. Finally, sup and inf represent the supremum and infimum respectively.

In order to be able to comprehensively observe the performance indicators of all test data in the INbreast and DDSM datasets, as shown in **Fig.5**, the statistical histogram distribution of the DSC scores obtained from the testing set is shown. It can be seen from **Fig.5** that the DSC values of the breast masses in the INbreast testing set are all higher than 0.8, and most of the breast masses have DSC values higher than 0.95. Although there are some breast masses with a DSC value lower than 0.8 in the DDSM testing set, most breast masses have a DSC value higher than 0.8, and there are also many breast masses with a DSC value higher than 0.95. Overall, the CasUNet segmentation model can extract effective features from mammography images, which can accurately segment breast masses.

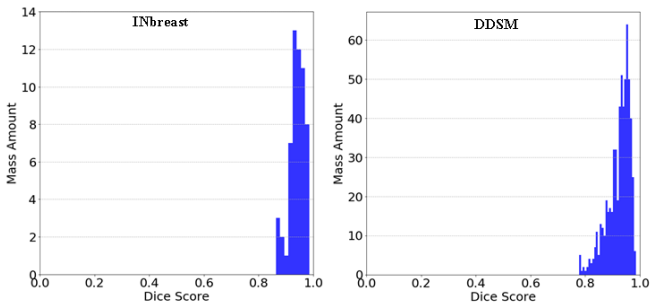

Fig. 5. DSC distributions of the INbreast and DDSM testing set

To verify the effectiveness of each component in the CasUNet segmentation architecture, we designed the ablation experiment shown in **Table 3** based on the INbreast dataset. **Table 3** shows the performance of each component gradually added based on UNet.

Comparing the experimental data of two adjacent rows in **Table 3**, it can be found that the various components proposed in this paper are conducive to the segmentation of breast masses. In particular, comparing the 5th and 6th rows of the experimental data in **Table 3**, we can find that based on the traditional data augmentation method, after further introducing the background migration data augmentation method, all indicators have been greatly improved. Specifically, IOU, DSC, REC, SPC increased by 2.7%, 1.7%, 1.9%, and 1.4%, respectively, and Haus reduced

by 5.0 pixels, which verifies the effectiveness of the background migration method from an experimental point of view.

Table 3. Ablation experiment. Note that, UNet6 represents the original UNet network with a depth of 6, and the number of output channels of its convolution layer doubles every time it is downsampled; The structure of $UNet_6$ is shown in **Table 2**, and the number of output channels of its convolutional layer increases by 32 every time downsampling; TN represents the truncation normalization data preprocessing method [29]; S1, S2 and S3 respectively represent image blocks of different scales, and their size relationships are shown in **Fig. 3**; TA represents the traditional data augmentation method; BM represents the background migration method; TA & BM indicates that two data augmentation methods, TA and BM, are used; SE represents the SeResNet module integrated on CasUNet; S1 & 2_MTP indicates that multi-stage cascaded training and prediction are performed using image blocks of two different scales, S1 and S2; S1 & 2_MTP_MA indicates that the mask image input to the second-stage model is randomly elastically deformed [26] to expand the training data of the second-stage model; Similarly, S1 & 2 & 3_MTP indicates that S1, S2, and S3 are used for multi-stage cascaded training and prediction; S1 & 2 & 3_MTP_MA indicates that the mask images input to the second and third stage models are randomly elastically deformed to expand the training data of the second and third stage models.

Methods	Para	IOU	DSC	REC	SPC	Haus
UNet6	5.4e7	0.825	0.902	0.920	0.884	35.55
UNet6_TN	5.4e7	0.827	0.903	0.936	0.870	35.30
$UNet_6$ _TN	0.7e7	0.839	0.909	0.925	0.884	34.85
$UNet_6$_TN_S1_TA	0.7e7	0.849	0.916	0.919	0.898	35.88
$UNet_6$_TN_S1_TA&BM	0.7e7	0.876	0.933	0.938	0.912	30.88
CasUNet_TN_S1_TA&BM	1.6e7	0.884	0.938	0.939	0.921	28.83
CasUNet_SE_TN_S1_TA&BM	1.6e7	0.884	0.937	0.941	0.932	27.75
CasUNet_SE_TN_S1&2_MTP_TA&BM	1.6e7	0.884	0.938	0.947	0.988	14.07
CasUNet_SE_TN_S1&2_MTP_MA_TA&BM	1.6e7	0.888	0.940	0.947	0.989	13.46
CasUNet_SE_TN_S1&2&3_MTP_TA&BM	1.6e7	0.885	0.939	0.942	0.995	9.357
CasUNet_SE_TN_S1&2&3_MTP_MA_TA&BM	1.6e7	0.891	0.942	0.943	0.996	8.911

Table 4. A comparison on the quantitative results of various mass detection methods. Please note that, "TM" indicates the traditional method, "DL" indicates the deep learning.

Methods	Datasets	Types	Images	IOU	DSC	REC	SPC	Haus
Cardoso et al. [12]	INbreast	TM	116	0.880	*	*	*	*
Dhungel et al. [15]	INbreast	DL	116	*	0.880	*	*	*
Dhungel et al. [14]	INbreast	DL	116	*	0.900	*	*	*
Al-antari et al. [17]	INbreast	DL	116	*	0.927	*	*	*
Zhu et al. [30]	INbreast	DL	116	*	0.910	*	*	*
Chen et al. [31]	INbreast	DL	116	*	0.937	*	*	*
Wang et al. [32]	INbreast	DL	116	*	0.911	*	*	*
Singh et al. [33]	INbreast	DL	116	*	0.940	*	*	*
Ours	**INbreast**	**DL**	**116**	**0.891**	**0.942**	**0.943**	**0.996**	**8.911**

Table 5. A comparison on the quantitative results of various mass detection methods. Please note that, "TM" indicates the traditional method, "DL" indicates the deep learning.

Methods	Datasets	Types	Images	IOU	DSC	REC	SPC	Haus
Pereira et al. [11]	DDSM	TM	160	0.792	*	*	*	*
Kashyap et al. [34]	DDSM	TM	300	*	0.910	*	*	*
Dhungel et al. [15]	DDSM	DL	158	*	0.870	*	*	*
Dhungel et al. [13]	DDSM	DL	158	*	0.890	*	*	*
Dhungel et al. [14]	DDSM	DL	158	*	0.900	*	*	*
Singh et al. [16]	DDSM	DL	567	*	0.944	0.927	0.987	*
Zhu et al.[30]	DDSM	DL	158	*	0.913	*	*	*
Chen et al. [31]	DDSM	DL	158	*	0.911	*	*	*
Wang et al. [32]	DDSM	DL	158	*	0.917	*	*	*
Ours	**DDSM**	**DL**	**10480**	**0.863**	**0.925**	**0.911**	**0.996**	**8.771**

To verify the superiority of the method proposed, we compare it with the breast mass segmentation method published in recent years. **Table 4** and **Table 5** respectively show the experimental comparison results of CasUNet on the INbreast and DDSM datasets.

It is not difficult to see from **Table 4** that on the INbreast dataset, the CasUNet method shows excellent performance whether it is compared with the traditional breast mass segmentation method or the deep learning-based breast mass segmentation method. For example, Cardoso et al. proposed a breast mass segmentation method based on energy optimization; and Al-antari et al. constructed a new depth network model, they use full-resolution convolutional network to segment breast masses. Similarly, as can be seen from **Table 5**, on the DDSM data set, the CasUNet segmentation method is superior to most

of the methods, but it is 1.9% lower than the DSC value obtained by the method proposed by Singh et al. Specifically, Singh et al. introduced a new method of breast mass segmentation based on conditional generative adversarial network. It should be noted that their experimental data was artificially selected, that is, they selected 567 malignant samples from the DDSM dataset.

4. CONCLUSION

This paper proposes a cascaded network architecture CasUNet. The depths of the six UNet sub-networks contained in CasUNet increase sequentially, so that the model can extract higher-level semantic features, which is beneficial to subsequent pixel-level classification. To solve the over-fitting problem caused by fewer training samples, we use the existing training samples as the basis to ensure the diversity of training samples through background migration. Furthermore, the multi-stage cascaded training and prediction method is beneficial to refine the segmentation results of breast masses. Experimental results show that compared with other existing methods, our proposed method has certain advantages.

REFERENCES

[1] F. Bray, J. Ferlay, I. Soerjomataram, R.L. Siegel, L.A. Torre, A. Jemal, Global cancer statistics 2018: GLOBOCAN estimates of incidence and mortality worldwide for 36 cancers in 185 countries, CA. Cancer J. Clin. 68 (2018) 394–424.

[2] L. Fan, K. Strasser-Weippl, J.-J. Li, J. St Louis, D.M. Finkelstein, K.-D. Yu, W.-Q. Chen, Z.-M. Shao, P.E. Goss, Breast cancer in China, Lancet Oncol. 15 (2014) e279–e289.

[3] X. Yan, R. Han, J. Zhou, H. Yu, M. Wu, Incidence, mortality and survival of female breast cancer during 2003-2011 in Jiangsu province, China, Chinese J. Cancer Res. 28 (2016) 321–329.

[4] C.D. Runowicz, C.R. Leach, N.L. Henry, K.S. Henry, H.T. Mackey, and P.A. Ganz, American Cancer Society/American Society of Clinical Oncology Breast Cancer Survivorship Care Guideline, CA. Cancer J. Clin. 66 (2016) 43–73.

[5] C.R. Smart, R.E. Hendrick, J.H. Rutledge III, R.A. Smith, Benefit of mammography screening in women ages 40 to 49 Years. Current evidence from randomized controlled trials, Cancer. 75 (1995) 1619–1626.

[6] E.D. Pisano, C. Gatsonis, E. Hendrick, M. Yaffe, J.K. Baum, S. Acharyya, E.F. Conant, L.L. Fajardo, L. Bassett, C. D'Orsi, R. Jong, M. Rebner, Diagnostic Performance of Digital versus Film Mammography for Breast-Cancer Screening, N. Engl. J. Med. 353 (2005) 1773–1783.

[7] P. Shanmugavadivu, V. Sivakumar, A Novel Technique for Mammogram Mass Segmentation Using Fractal Adaptive Thresholding, 2014.

[8] K. Divyadarshini, R. Vanithamani, Segmentation of mammographic masses using gray level thresholding, Int. J. Tomogr. Simul. 28 (2015) 22–32.

[9] Q. Abbas, M.E. Celebi, I.F. García, Breast mass segmentation using region-based and edge-based methods in a 4-stage multiscale system, Biomed. Signal Process. Control. 8 (2013) 204–214.

[10] E. Kozegar, M. Soryani, H. Behnam, M. Salamati, T. Tan, Mass Segmentation in Automated 3-D Breast Ultrasound Using Adaptive Region Growing and Supervised Edge-Based Deformable Model, IEEE Trans. Med. Imaging. 37 (2018) 918–928.

[11] D.C. Pereira, R.P. Ramos, M.Z. do Nascimento, Segmentation and detection of breast cancer in mammograms combining wavelet analysis and genetic algorithm, Comput. Methods Programs Biomed. 114 (2014) 88–101. https://doi.org/https://doi.org/10.1016/j.cmpb.2014.01.014.

[12] J.S. Cardoso, I. Domingues, H.P. Oliveira, Closed Shortest Path in the Original Coordinates with an Application to Breast Cancer, Int. J. Pattern Recognit. Artif. Intell. 29 (2014) 1555002.

[13] N. Dhungel, G. Carneiro, A.P. Bradley, Tree RE-weighted belief propagation using deep learning potentials for mass segmentation from mammograms, Int. Symp. Biomed. Imaging, 2015: pp. 760–763.

[14] N. Dhungel, G. Carneiro, A.P. Bradley, Deep Learning and Structured Prediction for the Segmentation of Mass in Mammograms BT - Medical Image Computing and Computer-Assisted Intervention -- MICCAI 2015, Springer International Publishing, Cham, 2015: pp. 605–612.

[15] N. Dhungel, G. Carneiro, A.P. Bradley, Deep structured learning for mass segmentation from mammograms, IEEE Int. Conf. Image Process., 2015: pp. 2950–2954.

[16] V.K. Singh, S. Romani, H.A. Rashwan, F. Akram, N. Pandey, M.M.K. Sarker, S. Abdulwahab, J. Torrents-Barrena, A. Saleh, M. Arquez, M. Arenas, D. Puig, Conditional Generative Adversarial and Convolutional Networks for X-ray Breast Mass Segmentation and Shape Classification BT - Medical Image Computing and Computer Assisted Intervention – MICCAI 2018, Springer International Publishing, Cham, 2018: pp. 833–840.

[17] M.A. Al-antari, M.A. Al-masni, M.-T. Choi, S.-M. Han, T.-S. Kim, A fully integrated computer-aided diagnosis system for digital X-ray mammograms via deep learning detection, segmentation, and classification, Int. J. Med. Inform. 117 (2018) 44–54.

[18] J. Hai, K. Qiao, J. Chen, H. Tan, J. Xu, L. Zeng, D. Shi, B. Yan, Fully Convolutional DenseNet with Multiscale Context for Automated Breast Tumor Segmentation, J. Healthc. Eng. 2019 (n.d.) 1–11.

[19] S. Li, M. Dong, G. Du, X. Mu, Attention Dense-U-Net for Automatic Breast Mass Segmentation in Digital Mammogram, IEEE Access. 7 (2019) 59037–59047.

[20] O. Ronneberger, P. Fischer, T. Brox, U-Net: Convolutional Networks for Biomedical Image Segmentation BT - Medical Image Computing and Computer-Assisted Intervention – MICCAI 2015, Springer International Publishing, Cham, 2015: pp. 234–241.

[21] J. Lemley, S. Bazrafkan, P. Corcoran, Smart Augmentation Learning an Optimal Data Augmentation Strategy, IEEE Access. 5 (2017) 5858–5869.

[22] A. Shrivastava, T. Pfister, O. Tuzel, J. Susskind, W. Wang, R. Webb, Learning from Simulated and Unsupervised Images through Adversarial Training, IEEE Conf. Comput. Vis. Pattern Recognit., 2017: pp. 2242–2251.

[23] H. Zhang, M. Cissé, Y.N. Dauphin, D. Lopez-Paz, mixup: Beyond Empirical Risk Minimization. BT - 6th International Conference on Learning Representations, ICLR 2018, Vancouver, BC, Canada, April 30 - May 3, 2018, Conference Track Proceedings, (2018).

[24] G. Thomas, Image segmentation using histogram specification, IEEE Int. Conf. Image Process., 2008: pp. 589–592.

[25] J. Hu, L. Shen, G. Sun, Squeeze-and-Excitation Networks, Comput. Vis. Pattern Recognit., 2018: pp. 7132–7141.

[26] P.Y. Simard, D. Steinkraus, J.C. Platt, Best practices for convolutional neural networks applied to visual document analysis. Proceedings., 2003: pp. 958–963.

[27] I.C. Moreira, I. Amaral, I. Domingues, A. Cardoso, M.J. Cardoso, J.S. Cardoso, INbreast: Toward a Full-field Digital Mammographic Database, Acad. Radiol. 19 (2012) 236–248.

[28] M. Heath, K. Bowyer, D. Kopans, R. Moore, W.P. Kegelmeyer, The digital database for screening mammography, Medical Physics Publishing, 2000: pp. 212–218.

[29] H. Cao, Breast mass detection in digital mammography based on anchor-free architecture, (2020).

[30] W. Zhu, X. Xiang, T.D. Tran, G.D. Hager, X. Xie, Adversarial deep structured nets for mass segmentation from mammograms, Int. Symp. Biomed. Imaging (ISBI 2018), IEEE, 2018: pp. 847–850.

[31] H. Li, D. Chen, W.H. Nailon, M.E. Davies, D. Laurenson, Improved Breast Mass Segmentation in Mammograms with Conditional Residual U-Net BT - Image Analysis for Moving Organ, Breast, and Thoracic Images, Springer International Publishing, Cham, 2018: pp. 81–89.

[32] R. Wang, Y. Ma, W. Sun, Y. Guo, W. Wang, Y. Qi, X. Gong, Multi-level nested pyramid network for mass segmentation in mammograms., Neurocomputing. 363 (2019) 313–320.

[33] V.K. Singh, H.A. Rashwan, S. Romani, F. Akram, N. Pandey, M.M.K. Sarker, A. Saleh, M. Arenas, M. Arquez, D. Puig, J. Torrents-Barrena, Breast tumor segmentation and shape classification in mammograms using generative adversarial and convolutional neural network, Expert Syst. Appl. 139 (2020) 112855.

[34] K.L. Kashyap, M.K. Bajpai, P. Khanna, Globally supported radial basis function based collocation method for evolution of level set in mass segmentation using mammograms, Comput. Biol. Med. 87 (2017) 22–37.